

Elsevier Editorial System(tm) for NIMA Proceedings
Manuscript Draft

Manuscript Number: NIMA_PROCEEDINGS-D-13-00121

Title: A Ring Imaging Cherenkov Detector for CLAS12

Article Type: Special Issue: VCI2013

Keywords: RICH; Ring Imaging Cherenkov; CLAS12; MAPMT; Multianode Photomultiplier Tube; H8500; Aerogel; Particle Identification

Corresponding Author: Miss Rachel Ann Montgomery,

Corresponding Author's Institution: University of Glasgow

First Author: Rachel Ann Montgomery

Order of Authors: Rachel Ann Montgomery

A Ring Imaging Cherenkov Detector for CLAS12

R.A. Montgomery^a, for the CLAS12-RICH collaboration.

^a *SUPA School of Physics & Astronomy, University of Glasgow, Kelvin Building, University Avenue, Glasgow, Scotland. G12 8QQ*

Abstract

The energy increase of Jefferson Lab's Continuous Electron Beam Accelerator Facility (CEBAF) to 12 GeV promises to greatly extend the physics reach of its experiments. This will include an upgrade of the CEBAF Large Acceptance Spectrometer (CLAS) to CLAS12, offering unique possibilities to study internal nucleon dynamics. For this excellent hadron identification over the full kinematical range of 3 - 8 GeV/c is essential. This will be achieved by the installation of a Ring Imaging Cherenkov (RICH) detector. A novel hybrid imaging design incorporating mirrors, aerogel radiators and Hamamatsu H8500 multianode photomultiplier tubes is proposed. Depending upon incident particle track angle, Cherenkov light will either be imaged directly or after two reflections and passes through the aerogel. The detector design is described, along with preliminary results on individual detector components tests and from recent testbeam studies.

Keywords: RICH, Ring Imaging Cherenkov, CLAS12, MAPMT, Multianode Photomultiplier Tube, H8500, Aerogel, Particle Identification

1. Jefferson Lab 12 GeV Upgrade and CLAS12

Jefferson Lab (JLab) (VA, USA) is currently undergoing an upgrade program which involves the increase in energy of its electron accelerator from 6 GeV to 12 GeV. The upgrade will also see the enhancement of detector capabilities in the existing experimental halls, including Hall B's CEBAF Large Acceptance Spectrometer (CLAS) [1] which will be upgraded to CLAS12 (see Fig. 1). CLAS12 will receive polarised beams of

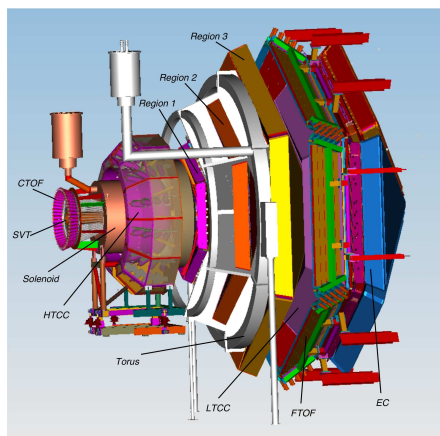


Figure 1: The CLAS12 detector [2]. The RICH detector will be positioned in place of the Low Threshold Cherenkov Counter (LTCC).

maximum energy 11 GeV and luminosity up to $10^{35} \text{ cm}^{-2} \text{ s}^{-1}$, providing a world-leading facility for the study of electron-nucleon scattering at these kinematics, with close to full angular

coverage. The physics program is extremely broad [2, 3], but in particular will focus upon three-dimensional imaging of the nucleon through the mapping of generalised parton and transverse momentum dependent distributions at high x_B with unprecedented precision. Other topics include quark hadronisation processes in the nuclear medium and spectroscopy studies. Efficient hadron identification is demanded across the entire kinematical range and, in particular, a π/K separation of $\sim 4\sigma$ at 8 GeV/c is the goal. Currently charged Particle Identification (PID) in CLAS12 is performed by Time-Of-Flight (TOF) detectors, Low and High Threshold Cherenkov Counters (LTCC, HTCC). These will not provide the necessary separation across the range of 3 - 8 GeV/c however and thus a RICH detector has been proposed for installation into the forward region of CLAS12, replacing the LTCC.

2. RICH Design

Since the RICH detector must fit into the original CLAS12 carriage there are several constraints imposed upon its design. Six radial sectors are required, each with projective geometry, limited gap depth of 1.2 m and $\sim 4.5 \text{ m}^2$ entrance windows. There is also a strict low material budget to minimise influence on the TOF detectors positioned behind the RICH. Simulation studies favour a hybrid imaging Cherenkov detector design incorporating aerogel radiators, visible light photon detectors, and a focussing mirror system [4, 5]. The focussing mirror system (see Fig. 2) will be used to reduce the detection area instrumented by photon detectors to $\sim 1 \text{ m}^2$ per sector, minimising costs and influence on the TOF system.

For forward scattered particles ($\theta < 12^\circ$) with momenta $p = 3 - 8 \text{ GeV}/c$ a proximity imaging method will be used, where the Cherenkov cone is imaged directly. For larger incident

Email address: r.montgomery.1@research.gla.ac.uk (R.A. Montgomery)

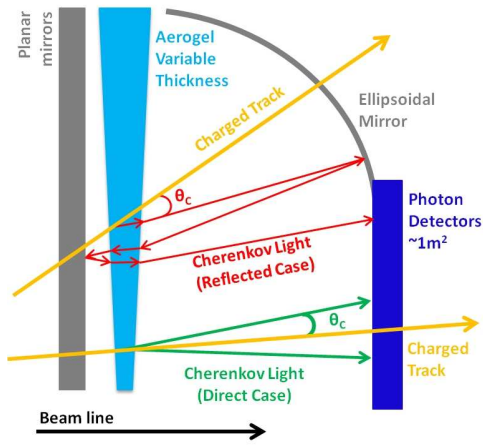


Figure 2: The hybrid RICH design concept - Cherenkov light is imaged directly for incident particle tracks of angles $< 12^\circ$, and after two reflections and passes through the aerogel radiator for particle tracks with incident angles between 12° and 35° .

particle angles of $12^\circ < \theta < 35^\circ$ and intermediate momenta of $p = 3 - 6 \text{ GeV}/c$ the Cherenkov light will be focussed by an elliptical mirror, followed by two further passes through the radiator material and a reflection from planar mirrors before detection. The Cherenkov light will be produced from a thicker amount of aerogel material than it will be reflected through, to compensate yield losses whilst obtaining a focalised ring. The case will also exist where Cherenkov rings are imaged partly by both the direct and reflected light cases simultaneously. For momenta below $3 \text{ GeV}/c$ the TOF system will provide the necessary π/K identification for polar angles up to 40° .

The RICH detector is simulated within the CLAS12 Geant4 framework. This also allows the development of pattern recognition algorithms, which involve maximum likelihood methods and ray tracing ansätze. Results from simulations imply that, to achieve the $\sim 4\sigma \pi/K$ goal at $8 \text{ GeV}/c$, of the order of 7 detected photons per ring are required in the direct light case.

Several characterisation studies of the individual RICH components are underway, a subset of which is described below.

3. Photon Detectors and the Hamamatsu H8500 MAPMT

There are several requirements limiting the choice of photon detector which have been confirmed through the simulation studies [4], for example the granularity of the photon detection plane. Due to the imaging aspect of the RICH and since multiple photon detectors will be tiled into large arrays, it is crucial that the photon detector provides an active area with minimal deadspace. The photon detector must also efficiently detect single photon level signals and, due to the aerogel radiator material, should be sensitive in visible light wavelengths.

MultiAnode PhotoMultiplier Tubes (MAPMTs) exist as promising candidates for the CLAS12 RICH and the currently selected photon detector is the flat-panel Hamamatsu H8500 MAPMT, which offers an adequate compromise between detector performance and cost. The H8500 MAPMT comprises an 8×8 array of pixels, each with dimensions $5.8 \text{ mm} \times 5.8 \text{ mm}$,

into an active area of $49.0 \text{ mm} \times 49.0 \text{ mm}$ and outer dimensions of $52.0 \text{ mm} \times 52.0 \text{ mm}$. Furthermore, the device has a very high packing fraction of 89%. Although the H8500 MAPMT is not advertised as the optimal MAPMT for single photon detection purposes, several units have been successfully used by the CLAS12-RICH group in a testbeam of a small-scale RICH prototype at the CERN T9 beamline in 2011. Results demonstrated sufficient capabilities of the H8500 to detect Cherenkov light. For example, a mean of ~ 11 photoelectrons per event (Cherenkov ring with 56.8% coverage) were obtained using a Novosibirsk tile of refractive index $n = 1.05$ and thickness 3 cm, and with a mixed hadron beam set at $10 \text{ GeV}/c$.

Laser scanning facilities have been setup for in-depth characterisations of MAPMTs. One topic which has been studied extensively includes the uniformity of the H8500 response. For example Fig. 3 shows the normalised single photoelectron signal efficiency response of an H8500 pixel and its surrounding area, obtained from a sub-mm precision laser scan. The signal efficiency is defined as the fraction of the single photoelectron distribution which lies above a 2σ pedestal cut. The pixel re-

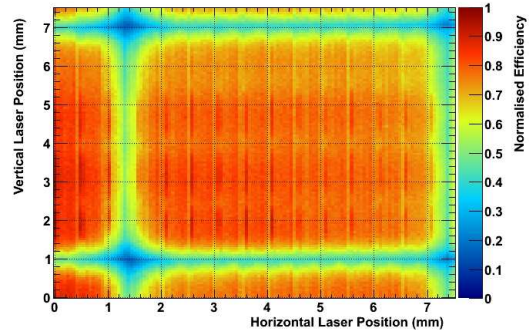


Figure 3: Normalised signal efficiency map of an H8500 pixel scanned in 0.04 mm steps, with a 633 nm laser beam focused to a diameter of 0.1 mm at single photoelectron light level.

sponse demonstrates a dependency upon the dynode structure of the MAPMT, where there exist periodic drops in signal efficiency when the laser strikes dynode support structures. The magnitudes of these drops are however small, with $\sim 5\%$ less relative signal efficiency compared to when the laser strikes dynode chain openings, and are not a concern for the CLAS12 RICH. Such studies are further described in [6], and they may also be used to study the PMT response in deadspace areas and to evaluate the true active areas of the pixels.

Further characterisation tests performed include studies devoted to: crosstalk, where magnitudes of $< 5\%$ are extracted; single photoelectron signal losses (defined as the fraction of the single photoelectron distribution lying below a 3σ pedestal threshold), which is minimised to $\sim 12\%$ through operation at -1075 V close to the suggested maximum operating voltage; response uniformity within pixel areas as a function of incident photon angles, which is unaltered up to tested angles of 30° and pixel to pixel gain variations, which again did not cause concern for the RICH.

117 **4. Prototype Studies at Testbeams**

118 Testbeam studies of a prototype RICH detector were per-
 119 formed in 2012 with the T9 beamline in the CERN-PS
 120 East Area, which provides secondary particles - mostly pi-
 121 ons and kaons - with selectable polarity and momenta from
 122 0 - 15 GeV/c. The prototype consisted of two setups, dedi-
 123 cated to study direct and reflected light imaging cases individu-
 124 ally. Gaseous Electron Multipliers (GEM) chambers were used
 125 for particle tracking and a beam threshold Cherenkov counter,
 126 which was provided in the T9 beam area, was set for kaons and
 127 pions to be below and above threshold respectively and used in
 128 offline kaon/pion separation analyses. Furthermore, a second
 129 smaller scale RICH prototype incorporating silicon photomul-
 130 tiplier arrays as photon detectors was included in the testbeams,
 131 however the results are not presented here.

132 For the direct light imaging case the prototype geometry
 133 was matched as close as possible to the CLAS12 RICH ge-
 134 ometry and a schematic of the setup is shown in Fig. 4.
 Novosibirsk aerogel tiles, of dimensions 6 cm × 6 cm, were

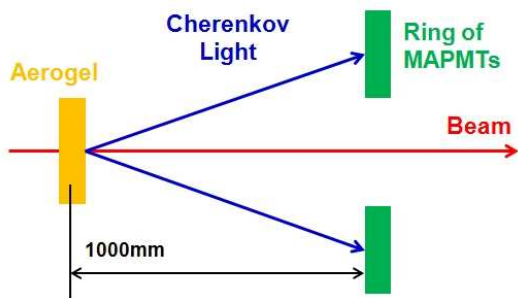


Figure 4: Diagram illustrating the proximity imaging setup of the testbeam prototype (side view).

135 used as Cherenkov radiators. Several thicknesses ($t = 2\text{ cm} - 4\text{ cm}$),
 136 transparencies and refractive indices ($n = 1.04 - 1.06$)
 137 were tested and their corresponding impact on the RICH proto-
 138 type performance are under study. The radiator was placed
 139 at 1 m from a ring of 28 H8500 MAPMTs, which could be
 140 moved radially for imaging of differing ring radii. Both stan-
 141 dard borosilicate and UV-extended window type MAPMTs
 142 were tested, to study yield differences and Rayleigh scattering
 143 resolution smearing effects. For readout of the MAPMTs the
 144 Multianode ReadOut Chip MAROC3 electronics [8] were used
 145 and, although the chip offers a sparsified readout mode, the en-
 146 tire charge spectrum of all channels was recorded to accurately
 147 study the MAROC3 and H8500 responses.

149 An example ring image obtained with the direct light setup is
 150 shown in Fig. 5, where the beam momentum was 8 GeV/c and
 151 the radiator had refractive index $n = 1.04$ and thickness 2 cm.
 152 Such images were used online as a check that ring properties
 153 behaved as expected - for example that radii increased with
 154 aerogel refractive index as is demonstrated in Fig. 6, where the
 155 refractive index is increased to $n = 1.06$. Moreover, in the on-
 156 line data analysis, π/K separation has already been observed.
 157 For example Fig. 7 displays Cherenkov ring radii distributions
 158 extracted from 3-parameter (ring centre and radius) ring fits to

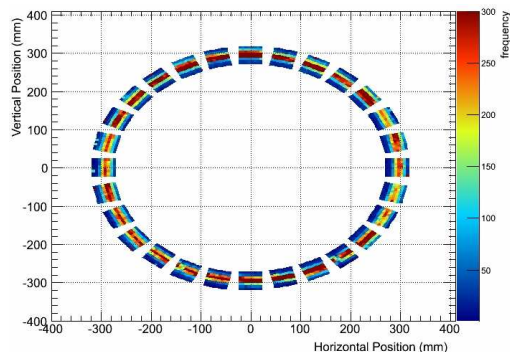


Figure 5: Direct light case testbeam prototype ring image, obtained beam momentum 8 GeV/c, aerogel refractive index 1.04 and thickness 2 cm.

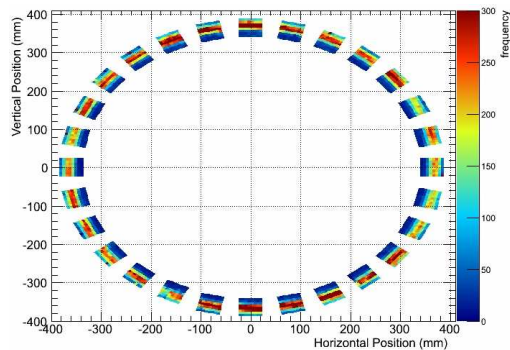


Figure 6: Direct light case testbeam prototype ring image, obtained beam momentum 8 GeV/c, aerogel refractive index 1.06 and thickness 2 cm.

159 the data obtained with a beam momentum 6 GeV/c, aerogel re-
 fractive index $n = 1.05$ and thickness 2 cm. The beam threshold

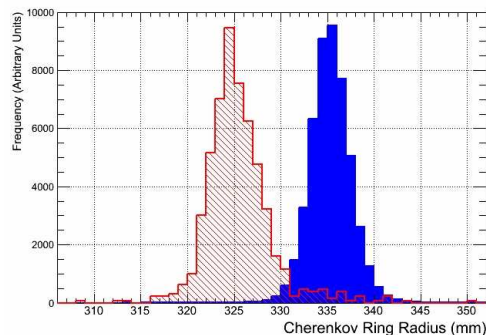


Figure 7: Cherenkov ring radii obtained for 6 GeV/c pions (blue/filled) and kaons (red/hatched), with the direct light testbeam setup and an aerogel radiator of $n = 1.05$ and thickness 2 cm.

Cherenkov counter was used as an offline kaon trigger, and cor-
 responding kaon and pion events are shown in the red/hatched
 and blue/filled histograms respectively. The kaon distribution
 has been subject to an amplitude scaling factor of 77, which is
 in rough agreement with the expected T9 beam composition at
 this momentum and negative polarity [7].

Currently investigations are underway to extract final light
 yield and ring resolution results, which are also converging with
 simulation comparisons. Due to the similarity of the geome-

170 tries, for the direct light imaging case the testbeam results may
 171 be extrapolated for CLAS12 RICH performance projections,
 172 and also be used for model inputs in the simulations.

173 The main aim of the reflected light case testbeam study was
 174 to investigate the Cherenkov light yield loss caused by multi-
 175 ple passes through aerogel. A schematic illustrating the test-
 beam prototype setup is shown in Fig. 8. A mirror, with focal

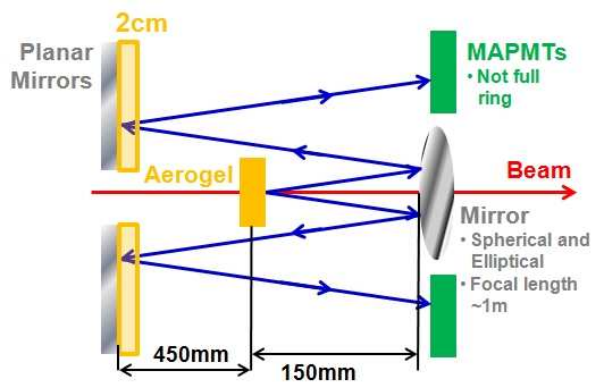


Figure 8: Diagram illustrating the setup of the reflected light case of the test-
 beam prototype (side view).

176 length ~ 1 m, was used to reflect Cherenkov light radiated from
 177 the aerogel along the beam to a wall of 8 planar mirrors with
 178 aerogel tiles, called absorbers, placed in front of them. The
 179 Cherenkov radiators were as in the direct light setup, but with
 180 increased thicknesses used (6 cm - 8 cm). The aerogel absorbers
 181 were $10\text{ cm} \times 10\text{ cm} \times 2\text{ cm}$ Novosibirsk tiles of varying trans-
 182 parencies and refractive index $n = 1.05$.

183 Fig. 9 shows an example ring image obtained with no ab-
 184 sorber tiles placed in front of the planar mirrors, a beam mo-
 185 mentum of $6\text{ GeV}/c$ and radiator refractive index of $n = 1.05$ and
 186 thickness 6 cm. For the reflected light measurements less than

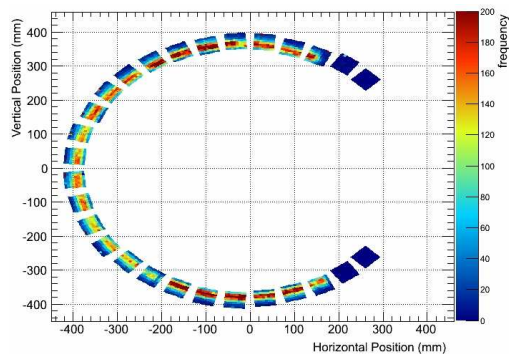


Figure 9: Reflected light case ring image, obtained with the testbeam prototype,
 without aerogel absorber tiles in front of the planar mirrors.

187 the full ring circumferences were instrumented, due to larger
 188 ring radii and setup shadowing effects. The corresponding im-
 189 age with absorbers before the planar mirrors is shown in Fig. 10.
 190 A lower Cherenkov yield (visible by colour scale) is extracted
 191 as a result of multiple passes through the aerogel absorbers.
 192 Nonetheless, the ring remains discernible and preliminary stud-

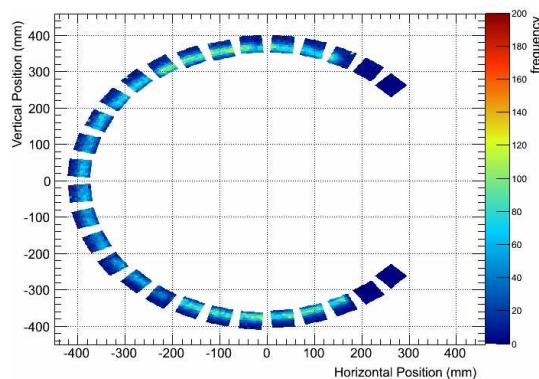


Figure 10: Reflected light case ring image, obtained with the testbeam proto-
 type, with aerogel absorber tiles in front of the planar mirrors.

194 ies indicate that the yield is sufficient to perform a likelihood
 195 pattern recognition analysis.

196 5. Summary

The installation of a RICH detector into CLAS12 for im-
 proved hadron identification over the $3-8\text{ GeV}/c$ momentum
 range will enhance its physics reach. A hybrid imaging de-
 sign has been proposed, incorporating both proximity and re-
 flected light imaging cases depending upon incident particle
 track angle. An in-depth characterisation program of individual
 detector components, including H8500 MAPMTs and aerogel
 radiators, is underway. Furthermore a large-scale testbeam
 prototype has been studied and currently extensive data analysis
 and simulation comparisons are ongoing, with further results
 on Cherenkov yield and ring resolutions to follow. From the
 prototype testbeam results it is decided that H8500 MAPMTs
 with standard Borosilicate glass windows only will be used in
 the CLAS12 RICH, since Cherenkov ring resolution degrada-
 tions were observed with UV-extended window types. The up-
 coming year will also include the construction and running of
 cosmic-ray prototypes for simulation validations and projected
 performance studies.

215 References

- 216 [1] B.A. Mecking *et al*, *The CEBAF large acceptance spectrometer (CLAS)*,
 Nucl. Instr. and Meth. A **503** (2003) 513.
- 217 [2] The CLAS Collaboration, *CLAS12 Technical Design Report*, ver-
 sion 5.1 (2008), http://www.jlab.org/Hall-B/clas12_tdr.pdf [Last Checked
 218 02/04/13].
- 219 [3] Hasch, D. *et al*, *Probing Strangeness in Hard Processes*,
arXiv:1202.1910v2 [hep-ex] (2012)
- 220 [4] M. Contalbrigo *et al*, *The CLAS12 large area RICH detector*, Nucl. Instr.
 and Meth. A **639** (2011) 302.
- 221 [5] A. El Alaoui *et al*, *A RICH detector for CLAS12 Spectrometer*, Physics
 Procedia **37** (2012) 773.
- 222 [6] R.A. Montgomery *et al*, *Multianode photomultiplier tube studies for*
imaging applications, Nucl. Instr. and Meth. A **695** (2012) 326.
- 223 [7] D.J. Simon *et al*, *Secondary Beams for Tests in the PS East Experimental*
Area, European Organisation for Nuclear Research, PS/PA Note 93-21,
 (1993) Revised version 4.8.93.
- 224 [8] S. Bliin *et al*, *MAROC, a generic photomultiplier readout chip*, JINST **5**
 (2010) C12007.